GEOLOGY | THE GEOLOGICAL SOCIETY OF AMERICA®

https://doi.org/10.1130/G48374.1

Manuscript received 8 September 2020
Revised manuscript received 30 November 2020
Manuscript accepted 2 December 2020

Published online 5 February 2021

Apatite nanoparticles in 3.46–2.46 Ga iron formations: Evidence for phosphorus-rich hydrothermal plumes on early Earth

Birger Rasmussen[1]*, Janet R. Muhling[1], Alexandra Suvorova[2] and Woodward W. Fischer[3]
[1]School of Earth Sciences, The University of Western Australia, Perth, Western Australia 6009, Australia
[2]Centre for Microscopy, Characterisation and Analysis, The University of Western Australia, Perth, Western Australia 6009, Australia
[3]Division of Geological and Planetary Sciences, California Institute of Technology, 1200 E. California Boulevard, Pasadena, California 91125, USA

ABSTRACT

Phosphorus is an essential nutrient that is thought to have regulated primary productivity in global oceans after the advent of oxygenic photosynthesis. The prime source of seawater phosphorus is regarded to be continental weathering of phosphate minerals. Ancient seawater phosphorus concentrations have been constrained using the phosphorus content of iron-rich chemical sediments—banded iron formations (BIFs); however, the removal processes and depositional phases remain unclear. Here we report that nanometer-sized apatite crystals (<500 nm) are ubiquitous in 3.46–2.46 Ga BIFs and cherts from the Kaapvaal (South Africa) and Yilgarn, and Pilbara (Western Australia) cratons. The apatite is uniformly dispersed in a chemical sediment comprising greenalite nanoparticles, which were encased in very early diagenetic silica cement that limited compaction and chemical reactions. The lack of organic carbon (below detection; <0.3 wt%) and absence of primary iron oxides implies that the phosphorus was not derived from the degradation of organic matter or seawater scavenging by oxide particles. Instead, the occurrence of apatite in sediments derived from hydrothermally sourced Fe^{2+} and SiO_2(aq) suggests that phosphorus too was derived from vent plumes. Today, seawater P is rapidly removed from vent fluids due to scavenging by oxidized Fe^{2+}. However, prior to the Great Oxidation Event (2.45–2.32 Ga), dissolved phosphorus released during anoxic alteration of seafloor basalts escaped the iron-oxidation trap. Our results point to the existence of a submarine hydrothermal flux of dissolved phosphorus that supplied nutrients to the early anoxic oceans. High amounts of seawater P may help to explain why phosphorus is ubiquitous in cell biology—it was not limiting during the origin and early evolution of life.

INTRODUCTION

Phosphorus plays core and wide-ranging roles in cell structure and biochemistry and is required for the growth and development of all organisms. Phosphorus availability also strongly influences the amounts and rates of photosynthesis, and consequently, its abundance in seawater plays a key role in the marine carbon cycle (Tyrrell, 1999; Ruttenberg, 2003; Planavsky et al., 2010). In modern oceans, phosphate is derived largely from terrestrial weathering and is removed by (1) biological uptake in the photic zone and sinking of biomass, and (2) adsorption on the surfaces of inorganic particles (commonly iron oxides) (Ruttenberg, 2003). The largest ultimate sink for seawater phosphate is the burial of authigenic apatite in marine sediments. Phosphate concentrations in seawater range from near zero in the photic zones to ~2.3 μM in the deep oceans—values too low for apatite precipitation in the water column to occur. However, beneath the sediment-water interface, the concentration of pore-water phosphate may increase by several orders of magnitude (to as much as 200 μM) during respiration and the release of organic-bound and adsorbed phosphorus; this leads to the growth of authigenic apatite (Ruttenberg, 2003).

Examination of ancient marine phosphorus concentrations has focused on its role in limiting primary productivity during Earth's early history (e.g., Bjerrum and Canfield, 2002). These studies have included measurement of the phosphorus content of banded iron formations (BIFs), which are organic-poor, iron-rich chemical sediments that, according to traditional models, were deposited as ferric oxide and/or hydroxide particles following oxidation of dissolved Fe^{2+} in upwelling hydrothermal plumes (Konhauser et al., 2017). In this model, the settling iron-oxide particles strongly adsorbed phosphorus from the water column, as in modern hydrothermal plumes (Wheat et al., 1996), forming extensive seafloor deposits that preserve a record of seawater phosphorus concentrations through Precambrian time (Bjerrum and Canfield, 2002; Planavsky et al., 2010). Because phosphorus adsorbs predictably onto the surfaces of iron-oxide particles, preserving a strong correlation between iron and phosphorus contents in modern hydrothermal sediments, the P/Fe ratios of BIFs have been used to calculate ancient oceanic phosphorus concentrations (Bjerrum and Canfield, 2002; Planavsky et al., 2010). Depending on the competitive role of silica adsorption onto iron-oxide particles, estimates of phosphorus concentration range from 10%–25% (no silica) (Bjerrum and Canfield, 2002) to 400% (2.2 mM silica) (Planavsky et al., 2010) of present-day concentrations for the deep sea.

Recent studies have revealed the presence of iron-rich nanoparticles of the Fe(II)-silicate greenalite [ideal formula $(Fe)_3Si_2O_5(OH)_4$] in BIFs from Australia and South Africa (Rasmussen et al., 2015, 2017, 2019a, 2019b; Johnson et al., 2018; Muhling and Rasmussen, 2020). Their microfabric and association with sedimentary lamination suggest that greenalite particles, rather than iron oxide/hydroxide particles, were the original precipitates (Rasmussen et al., 2019a). These observations from the ancient rock record are supported by experimental data that indicate that Fe(II)-silicate precipitation is favored under the anoxic ferruginous conditions inferred to have existed in early Precambrian oceans (Tosca et al., 2016, 2019). If correct, these results raise questions about the role of iron oxides in the

*E-mail: Birger.Rasmussen@uwa.edu.au

CITATION: Rasmussen, B., et al., 2021, Apatite nanoparticles in 3.46–2.46 Ga iron formations: Evidence for phosphorus-rich hydrothermal plumes on early Earth: Geology, v. 49, p. 647–651, https://doi.org/10.1130/G48374.1

removal of dissolved phosphorus and the phosphorus concentration in the early oceans.

METHODS AND SAMPLE DETAILS

We employed high-resolution transmission electron microscopy (TEM) methods (see the Supplemental Material[1]) to identify and characterize the earliest-formed phosphate phases in 3.46–2.46 Ga BIFs from the Archean Pilbara and Yilgarn cratons (Western Australia) and the Kaapvaal craton (South Africa) (Table S1 in the Supplemental Material). BIFs from these cratons are among the least-deformed and least-metamorphosed successions in the early Precambrian rock record. Most of the samples are from drill cores that accessed regions below the zone of modern weathering and are distal to iron ore mines.

RESULTS

Fe(II)-Silicate Nanoparticles in Laminated Chert

Laminated ferruginous chert was targeted because it preserves sedimentological and mineralogical information about the origin of BIFs. Each chert bed examined contained minute (<1-μm-long) particles of greenalite and/or stilpnomelane that are associated with, and locally define, sedimentary lamination and occur in chert that displays dehydration structures (Rasmussen et al., 2015, 2017, 2019a, 2019b). The uniform distribution within laminae and random orientation of the greenalite nanoparticles, as well as the high initial porosity (minus chert) of the sediment, are characteristic features of modern clay-rich muds that indicate deposition by settling from suspension (Rasmussen et al., 2019a). The minute size of the greenalite particles is typical of seawater precipitates in long-traveled hydrothermal plumes as well as precipitates produced from low-temperature clay synthesis experiments (Tosca et al., 2016). The preservation of depositional fabrics by chert indicates that the greenalitic muds were encased in silica cement on or just below the seafloor, transforming the once-porous mud, originally comprising 80%–95% water, into a greenalite-bearing chert (Rasmussen et al., 2019a).

Apatite Nanoparticles

Apatite nanoparticles were found in all of the samples of laminated chert (Table S1). The particles are elongate (between 10–500 nm long) (Fig. 1) and composed of Ca, P, O, and minor F (Fig. S1 in the Supplemental Material). High-resolution TEM imaging showed that the elongate particles are randomly oriented and uniformly distributed throughout the silica-cemented greenalite mud. The phosphate particles occur adjacent to iron-silicate nanoparticles or in the interstitial chert cement (Fig. 1) but were not identified in diagenetic shrinkage structures that truncate the greenalite sediment.

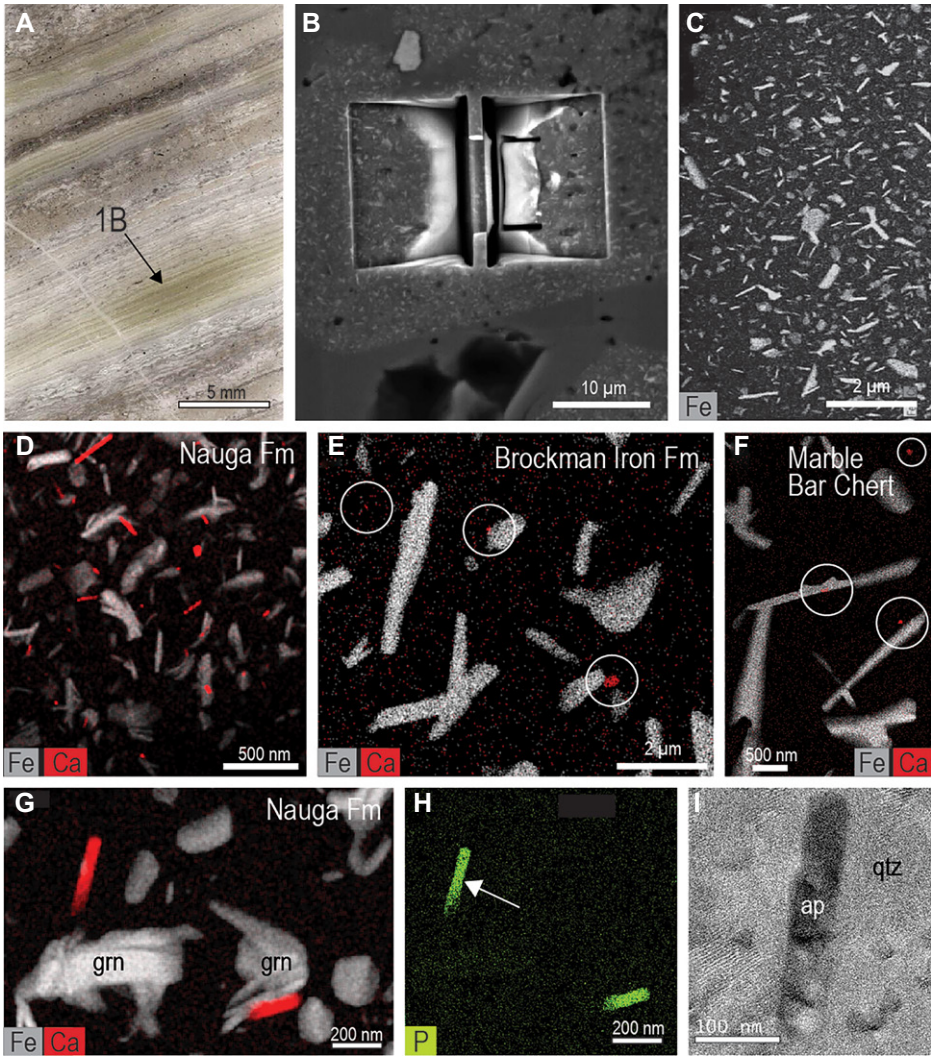

Figure 1. (A) Polished thin section containing greenalite-rich chert (arrow). (B) Back-scattered electron image of pit cut by focused ion beam (FIB) from chert with abundant greenalite nanoparticles. (C) Iron (gray) element map from X-ray spectroscopy of transmission electron microscopy (TEM) foil cut by FIB from chert showing randomly oriented greenalite particles. (D–G) Fe and Ca element maps showing greenalite (grn) laths (gray) and apatite nanoparticles (red) in cherts from the upper Nauga Formation of South Africa (ca. 2.55 Ga) (D,G), Brockman Iron Formation of Western Australia (ca. 2.48 Ga) (E), and Marble Bar Chert of Western Australia (ca. 3.46 Ga) (F). Small white circles in E and F surround minute apatite nanoparticles. (H) Phosphorus element map for G. (I) TEM image of apatite (ap) particle in H (see arrow) (qtz—quartz).

Smaller grains were unstable and damaged under the high-energy electron beam. However, high-resolution analysis of two larger particles (Fig. S2) allowed *d*-spacings to be measured from diffractograms; these are consistent with fluorapatite (Table S2) [ideal formula $Ca_5(PO_4)_3F$]. The original phase is uncertain but may have been carbonate fluorapatite [$Ca_5(PO_4,CO_3)_3F$]—the most common authigenic phosphate phase in marine sediments—that subsequently recrystallized to apatite. Nanometer-scale analysis and element mapping by TEM of the apatite-bearing cherts shows that reduced carbon contents are below detection (~0.3 wt%).

DISCUSSION

Source of Phosphorus

Apatite in marine sediments is generally thought to have formed during early diagenesis (Ruttenberg, 2003). Sediment pore-water profiles indicate that apatite (as carbonate fluorapatite) starts to precipitate immediately below the seafloor, tied to the remineralization of organic matter, which increases pore-water phosphate concentrations. However, BIFs are

[1]Supplemental Material. Methods, Figures S1 and S2, and Tables S1–S3. Please visit https://doi.org/10.1130/GEOL.S.13584914 to access the supplemental material, and contact editing@geosociety.org with any questions.

renowned for their very low organic carbon content (e.g., ~0.01 wt% in Transvaal BIFs on the Kaapvaal craton) (Konhauser et al., 2017). This is confirmed by our nanometer-scale analysis of the apatite-bearing cherts (<0.3 wt%). So, if organic matter were the source of phosphorus for apatite precipitation, it must have vanished in each sample that we examined, which would require that the original oxidized (e.g., ferric oxides/hydroxides) and reduced (organic matter) phases were consumed.

Another source of phosphorus in modern marine sediments are ferric oxide/hydroxide particles (Ruttenberg, 2003), which strongly scavenge dissolved phosphate from seawater (Wheat et al., 1996). Subsequent redox cycling of ferric oxides/hydroxides in the presence of organic matter liberates adsorbed phosphorus, increasing pore-water phosphate concentrations. Scavenging of phosphorus by ferric oxide/hydroxide particles produces a strong correlation between phosphorus and iron in hydrothermal plumes and precipitates (Wheat et al., 1996), which may be preserved during burial despite mineralogical transformations (Planavsky et al., 2010).

Published geochemical data sets (Table S3) show that there is a strong correlation between the phosphorus and iron contents of hydrothermal sediments from the East Pacific Rise (Fig. 2A). However, data from the late Archean–early Paleoproterozoic Transvaal (Kaapvaal craton) and Hamersley (Pilbara craton) provinces show that there is no such relationship in major BIFs (Figs. 2B–2D). Either the correlation between phosphorus and iron contents was destroyed after deposition, in which case the P/Fe ratios of BIFs do not accurately record seawater phosphorus concentrations, or iron-oxide scavenging did not control phosphorus removal from the water column.

Our observations support the latter interpretation, namely that the precursor sediment was not an iron oxide/hydroxide precipitate, but rather an Fe(II)-rich mud comprising greenalite nanoparticles. If correct, then the presence of apatite in greenalite-rich sediments, which were essentially derived from vent plumes enriched in Fe^{2+} and SiO_2(aq), would suggest that a proportion of the phosphorus was also sourced from vent plumes. This interpretation is supported by recent experimental work, which indicates that significant amounts of phosphate may be released during the anoxic submarine weathering of basalts. It has been argued that hydrothermal seafloor alteration of basalts can potentially release up to 90% of the phosphorus bound in volcanic glass (Staudigel and Hart, 1983; Nisbet, 1986; Gernon et al., 2016). Whereas in modern hydrothermal plumes the oxidation of reduced iron rapidly removes marine phosphorus, rendering ocean ridge systems a net phosphorus sink, prior to the Great Oxidation Event (GOE) (2.45–2.32 Ga), reduced iron emitted at vent systems was not oxidized and therefore did not trap dissolved phosphorus around seafloor vent systems.

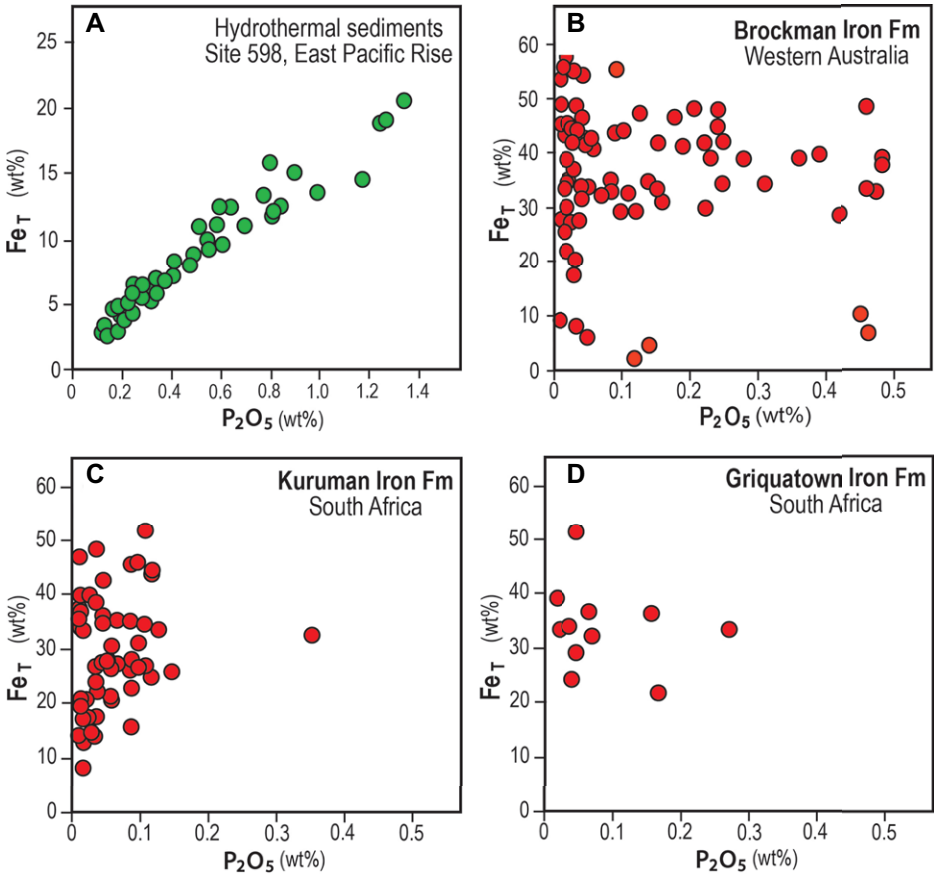

Figure 2. Total iron (Fe_T) plotted against P_2O_5 concentration (wt%) for red, iron oxide–bearing hydrothermal sediments from Deep Sea Drilling Project Site 598 on the East Pacific Rise (A), ca. 2.48 Ga Brockman Iron Formation of Western Australia (B), ca. 2.46 Ga Kuruman Iron Formation of South Africa (C), and ca. 2.45 Ga Griquatown Iron Formation of South Africa (D). Data are from Trendall and Blockley (1970), Klein and Beukes (1989), Beukes and Klein (1990) and Planavsky et al. (2010).

Apatite Precipitation

The presence of apatite nanoparticles in hydrothermal sediments devoid of organic matter and iron oxides argues against diagenetic phosphate enrichment in sediment pore waters, as occurs in modern shelf sediments (Ruttenberg, 2003). Our observations suggest that a precursor calcium phosphate phase coprecipitated with greenalite in plume-modified seawater and was deposited during the settling of larger Fe(II)-silicate particles. The absence of Fe(II)-phosphates (vivianite) may reflect low Fe^{2+} concentrations due to the rapid precipitation of greenalite (cf. Johnson et al., 2020). The growth of apatite nanoparticles in plume-dominated seawater requires that phosphorus concentrations be high enough to nucleate and precipitate a calcium phosphate phase. The phosphorus content of modern plumes or seawater is too low to accomplish this, and because calcium phosphate solubility in seawater is dictated by phosphate rather than calcium concentrations (Bentor, 1980; Jahnke, 1984), these observations indicate that the phosphate content of plume-dominated seawater was much higher than it is now. How high is uncertain because the solubility of calcium phosphate salts is notoriously complex and depends on both mineral and solution chemistry (Atlas and Pytkowicz, 1977; Morse and Casey, 1988). Indeed, some evidence suggests that much apatite formation may proceed through the production of kinetically labile precursors like octacalcium phosphate or other amorphous phases (Morse and Casey, 1988; Oxmann and Schwendenmann, 2014).

Present-day apatite growth has been inferred in marine sediments from continental margins, where pore-water phosphate concentrations range from 20 μM to >200 μM (Ruttenberg, 2003). These values provide estimates for the concentrations required to produce apatite in complex solutions like seawater and are consistent with evidence that phosphate concentrations must rise substantially above seawater values for calcium phosphate phases to nucleate and grow (Krajewski et al., 1994;

Oxmann and Schwendenmann, 2014). Assuming the calcium concentration of >2.45 Ga plume-modified seawater was within half to twice that of modern seawater (Blättler et al., 2016), estimates indicate that dissolved P was between 10 μM and 100 μM, at least 5×—and perhaps as much as 50×—that of today in the deep oceans.

Carbonate chemistry can also play a role in the solubility of apatite phases, with as much as a hundred-fold rise in solubility with increasing carbonate ion concentration (Jahnke, 1984). Based on this estimate, it has been argued that the solubility of apatite phases in Precambrian seawater was substantially higher than that of today (Planavsky et al., 2010). If correct, then one can infer from our observations that environmental phosphorus concentrations were significantly higher than at any other time in Earth history.

IMPLICATIONS

The ubiquity of apatite nanoparticles in >2.46 Ga chemical sediments largely derived from vent plumes indicates that the alteration of seafloor basalts was potentially a source of phosphorus in anoxic oceans on early Earth. Although the precipitates have been identified only in plume-dominated sediments, the existence of a large continuous flux of hydrothermal phosphorus at concentrations >10 μM (or even >100 μM) implies that the global oceans may also have been enriched in phosphorus. At the higher phosphorus concentrations estimated for Archean oceans (10–100 μM), it follows that biological productivity was unlikely to have been constrained by phosphorus availability. In turn, this suggests that primary production was limited by other chemical species like fixed nitrogen or electron donors—the latter may have controlled productivity prior to the advent of water-oxidizing (i.e., oxygenic) photosynthesis (Kharecha et al., 2005; Ward et al., 2019).

While the timing of the evolution of oxygenic photosynthesis within the Cyanobacteria remains an open question, one set of hypotheses holds that this occurred shortly before the GOE (Fischer et al., 2016; Soo et al., 2017). If that notion is correct, our results indicate that the ecosystems into which oxygenic photosynthesis would emerge were far richer in phosphorus than even those that support the most productive areas of the Earth's surface today.

Our results may also have implications for the "phosphate problem" concerning the development of life: that is, why did life select phosphorus for so many essential biochemical processes, including the manufacture of genetic material, when soluble phosphorus is so scarce? While there are aspects of its chemistry that are well suited to biological tasks (Westheimer, 1987; Benner and Hutter, 2002), our observations highlight another reason why phosphate was so readily integrated into a range of cellular functions: it was abundant in Earth's early oceans.

ACKNOWLEDGMENTS

This work was supported by Australian Research Council grants DP140100512 (to Rasmussen) and DP190102237 (to Rasmussen and Muhling). Support for Fischer was provided by the Simons Foundation Collaboration on the Origins of Life (New York, USA). Focused ion beam and TEM analyses were performed at the Centre for Microscopy, Characterisation and Analysis at The University of Western Australia, a node of Microscopy Australia funded from university and government sources. The manuscript benefitted from comments by Huan Cui and two anonymous journal reviewers.

REFERENCES CITED

Atlas, E.L., and Pytkowicz, R.M., 1977, Solubility behavior of apatites in seawater: Limnology and Oceanography, v. 22, p. 290–300, https://doi.org/10.4319/lo.1977.22.2.0290.

Benner, S.A., and Hutter, D., 2002, Phosphates, DNA, and the search for nonterrean life: A second generation model for genetic molecules: Bioinorganic Chemistry, v. 30, p. 62–80, https://doi.org/10.1006/bioo.2001.1232.

Bentor, Y.K., 1980, Phosphorites—The unsolved problems, *in* Bentor, Y.K., ed., Marine Phosphorites—Geochemistry, Occurrence, Genesis: SEPM (Society for Sedimentary Geology) Special Publication 29, p. 3–18, https://doi.org/10.2110/pec.80.29.0003.

Beukes, N.J., and Klein, C., 1990, Geochemistry and sedimentology of a facies transition from microbanded to granular iron-formation in the early Proterozoic Transvaal Supergroup, South Africa: Precambrian Research, v. 47, p. 99–139.

Bjerrum, C.J., and Canfield, D.E., 2002, Ocean productivity before about 1.9 Gyr ago limited by phosphorus adsorption onto iron oxides: Nature, v. 417, p. 159–162, https://doi.org/10.1038/417159a.

Blättler, C.L., Kump, L.R., Fischer, W.W., Paris, G., Kasbohm, J.J., and Higgins, J.A., 2016, Constraints on ocean carbonate chemistry and pCO_2 in the Archaean and Paleoproterozoic: Nature Geoscience, v. 10, p. 41–45, https://doi.org/10.1038/ngeo2844.

Fischer, W.W., Hemp, J., and Johnson, J.E., 2016, Evolution of oxygenic photosynthesis: Annual Review of Earth and Planetary Sciences, v. 44, p. 647–683, https://doi.org/10.1146/annurev-earth-060313-054810.

Gernon, T.M., Hincks, T.K., Tyrrell, T., Rohling, E.J., and Palmer, M.R., 2016, Snowball Earth ocean chemistry driven by extensive ridge volcanism during Rodinia breakup: Nature Geoscience, v. 9, p. 242–248, https://doi.org/10.1038/ngeo2632.

Jahnke, R.A., 1984, The synthesis and solubility of carbonate fluorapatite: American Journal of Science, v. 284, p. 58–78, https://doi.org/10.2475/ajs.284.1.58.

Johnson, B.R., Tostevin, R., Gopon, P., Wells, J., Robinson, S.A., and Tosca, N.J., 2020, Phosphorus burial in ferruginous SiO_2-rich Mesoproterozoic sediments: Geology, v. 48, p. 92–96, https://doi.org/10.1130/G46824.1.

Johnson, J.E., Muhling, J.R., Cosmidis, J., Rasmussen, B., and Templeton, A.S., 2018, Low-Fe(III) greenalite was a primary mineral from Neoarchean oceans: Geophysical Research Letters, v. 45, p. 3182–3192, https://doi.org/10.1002/2017GL076311.

Kharecha, P., Kasting, J., and Siefert, J.A., 2005, Coupled atmosphere-ecosystem model of the early Archean Earth: Geobiology, v. 3, p. 53–76, https://doi.org/10.1111/j.1472-4669.2005.00049.x.

Klein, C., and Beukes, N.J., 1989, Geochemistry and sedimentology of a facies transition from limestone to iron-formation deposition in the Early Proterozoic Transvaal Supergroup, South Africa: Economic Geology, v. 84, p. 1733–1774.

Konhauser, K.O., et al., 2017, Iron formations: A global record of Neoarchean to Paleoproterozoic environmental history: Earth-Science Reviews, v. 172, p. 140–177, https://doi.org/10.1016/j.earscirev.2017.06.012.

Krajewski, K.P., et al., 1994, Biological processes and apatite formation in sedimentary environments: Eclogae Geologicae Helvetiae, v. 87, p. 701–745.

Morse, J.W., and Casey, W.H., 1988, Ostwald processes and mineral paragenesis in sediments: American Journal of Science, v. 288, p. 537–560, https://doi.org/10.2475/ajs.288.6.537.

Muhling, J.R., and Rasmussen, B., 2020, Widespread deposition of greenalite to form banded iron formations before the Great Oxidation Event: Precambrian Research, v. 339, 105619, https://doi.org/10.1016/j.precamres.2020.105619.

Nisbet, E.G., 1986, RNA and hot-water springs: Nature, v. 322, p. 206, https://doi.org/10.1038/322206a0.

Oxmann, J.F., and Schwendenmann, L., 2014, Quantification of octacalcium phosphate, authigenic apatite and detrital apatite in coastal sediments using differential dissolution and standard addition: Ocean Science, v. 10, p. 571–585, https://doi.org/10.5194/os-10-571-2014.

Planavsky, N.J., Rouxel, O.J., Bekker, A., Lalonde, S.V., Konhauser, K.O., Reinhard, C.T., and Lyons, T.W., 2010, The evolution of the marine phosphate reservoir: Nature, v. 467, p. 1088–1090, https://doi.org/10.1038/nature09485.

Rasmussen, B., Krapež, B., Muhling, J.R., and Suvorova, A., 2015, Precipitation of iron silicate nanoparticles in early Precambrian oceans marks Earth's first iron age: Geology, v. 43, p. 303–306, https://doi.org/10.1130/G36309.1.

Rasmussen, B., Muhling, J.R., Suvorova, A., and Krapež, B., 2017, Greenalite precipitation linked to the deposition of banded iron formations downslope from a late Archaean carbonate platform: Precambrian Research, v. 290, p. 49–62, https://doi.org/10.1016/j.precamres.2016.12.005.

Rasmussen, B., Muhling, J.R., and Fischer, W.W., 2019a, Evidence from laminated chert in banded iron formations for deposition by gravitational settling of iron-silicate muds: Geology, v. 47, p. 167–170, https://doi.org/10.1130/G45560.1.

Rasmussen, B., Muhling, J.R., Tosca, N.J., and Tsikos, H., 2019b, Evidence for anoxic shallow oceans at 2.45 Ga: Implications for the rise of oxygenic photosynthesis: Geology, v. 47, p. 622–626, https://doi.org/10.1130/G46162.1.

Ruttenberg, K.C., 2003, The global phosphorus cycle, *in* Schlesinger, W.H., ed., Treatise on Geochemistry, Volume 8: Biogeochemistry: Elsevier, p. 585–643, https://doi.org/10.1016/B0-08-043751-6/08153-6.

Soo, R.M., Hemp, J., Parks, D.H., Fischer, W.W., and Hugenholtz, P., 2017, On the origins of oxygenic photosynthesis and aerobic respiration in Cyanobacteria: Science, v. 355, p. 1436–1440, https://doi.org/10.1126/science.aal3794.

Staudigel, H., and Hart, S.R., 1983, Alteration of basaltic glass: Mechanisms and significance for the oceanic crust-seawater budget: Geochimica

et Cosmochimica Acta, v. 47, p. 337–350, https://doi.org/10.1016/0016-7037(83)90257-0.
Tosca, N.J., Guggenheim, S., and Pufahl, P.K., 2016, An authigenic origin for Precambrian greenalite: Implications for iron formation and the chemistry of ancient seawater: Geological Society of America Bulletin, v. 128, p. 511–530, https://doi.org/10.1130/B31339.1.
Tosca, N.J., Jiang, C.Z., Rasmussen, B., and Muhling, J., 2019, Products of the iron cycle on the early Earth: Free Radical: Medicine and Biology, v. 140, p. 138–150, https://doi.org/10.1016/j.freeradbiomed.2019.05.005.
Trendall, A.F., and Blockley, J.G., 1970, The Iron-Formations of the Precambrian Hamersley Group, Western Australia: Perth, Geological Survey of Western Australia, Bulletin 119, 366 p.
Tyrrell, T., 1999, The relative influences of nitrogen and phosphorus on oceanic primary production: Nature, v. 400, p. 525–531, https://doi.org/10.1038/22941.
Ward, L.M., Rasmussen, B., and Fischer, W.W., 2019, Primary productivity was limited by electron donors prior to the advent of oxygenic photosynthesis: Journal of Geophysical Research: Biogeosciences, v. 124, p. 211–226, https://doi.org/10.1029/2018JG004679.
Westheimer, F.H., 1987, Why nature chose phosphates: Science, v. 235, p. 1173–1178, https://doi.org/10.1126/science.2434996.
Wheat, C.G., Feely, R.A., and Mottl, M.J., 1996, Phosphate removal by oceanic hydrothermal processes: An update of the phosphorus budget in the oceans: Geochimica et Cosmochimica Acta, v. 60, p. 3593–3608, https://doi.org/10.1016/0016-7037(96)00189-5.

Printed in USA